Computational Studies on Metathetical and Redox Processes of HOCl in the Gas Phase. 1. Reactions with H, O, HO, and HO_2

Z. F. Xu and M. C. Lin*

Department of Chemistry, Emory University, Atlanta, Georgia 30322

Received: June 1, 2009; Revised Manuscript Received: June 19, 2009

The potential energy surfaces of four reactions including (a) HOCl + H, (b) HOCl + O, (c) HOCl + HO, (d) HOCl + HO_2, have been studied by the CCSD(T)/aug-cc-pVTZ//CCSD/aug-cc-pVDZ, CCSD(T)/aug-cc-pVTZ//CCSD/cc-pVDZ, and CCSD(T)/6-311+G(3df,2p)//BH&HLYP/6-311+G(3df,2p) levels of theory. For both HOCl + H and HOCl + O, the direct Cl-abstraction channels take place via the lowest energy barriers; for both HOCl + HO and HOCl + HO_2, the lowest energy barrier channels are the indirect H-abstraction reactions by HO_x ($x = 1, 2$) via long-lived reaction intermediates. The rate constants for the low barrier channels have been calculated in the temperature range 200−3000 K by statistical theory. The predicted rate constants for HOCl + H and HOCl + HO are in good agreement with experimental results whereas that for HOCl + O was found to be in disagreement with the majority of available experimental data, suggesting a need for further improvement in theory and/or experiment.

1. Introduction

Hypochlorous acid (HOCl) plays an important role not only in atmospheric chemistry[1] but also in the combustion of ammonium perchlorate (AP), an important propellant today.[2] In the former case, HOCl is considered to be a temporary reservoir of atmospheric chlorine because it can be photolyzed by sunlight

$$\mathrm{HOCl} + h\nu \rightarrow \mathrm{HO} + \mathrm{Cl}$$

HOCl can also react with atmospheric radical species, such as H, O(^{3}P), HO, HO_2, etc., yielding fragments that can lead to ozone destruction. In the combustion of AP, following the sublimation of AP concurrently producing ammonia (NH_3) and perchloric acid ($HClO_4$),[3a] the acid decomposition in the gas phase produces initially ClO_3 and OH radicals. The reactive chlorine trioxide (ClO_3) can be rapidly converted to ClO and HOCl by reduction reactions involving OH and NH_x ($x = 1-3$) in high temperature media. Consequently, the reactions of HOCl with the active radicals H, O(^{3}P), HO, and HO_2 can be expected to take place and play a significant role in the chemistry of the AP propulsion process.[3b]

In the literature, there exists only a small number of the experimental studies on the kinetics and mechanisms of HOCl reactions with H, O, HO, and HO_2 in the past thirty years.[4−11] In 1988, Ennis and Birks[4] measured the rate constants of HOCl reactions with H and HO at 298 K using a low-pressure mass spectrometry-resonance fluoresence discharge flow system. They determined k(HOCl+H) and k(HOCl+HO) to be (5.0 ± 1.4) × 10^{-12} cm^3 molecule^{-1} s^{-1} and (1.7−9.5) × 10^{-13} cm^3 molecule^{-1} s^{-1}, respectively. In 1993, Vogt and Schindler[5] carried out a kinetic study on the reactions of HOCl with H, F and Cl at room temperature in a discharge flow system. k(HOCl+H) was measured to be (3.5 ± 0.7) × 10^{-12} cm^3 molecule^{-1} s^{-1}, which is in reasonable agreement with Ennis and Birks' value.[4] For the reaction of HOCl with O(^{3}P), Vogt, Schindler, and co-workers[6] in 1992 and 1996[7] measured its rate constants with the values (1.3 ± 0.2) × 10^{-13} cm^3 molecule^{-1} s^{-1} at room temperature and (1.7 ± 0.3) × 10^{-13} cm^3 molecule^{-1}s^{-1} at 213−298 K, respectively. In addition, on the basis of the above experimental values Atkinson et al.[8] recommended in 1997 the rate constant expressions, k(HOCl+HO) = 3.0 × 10^{-12} exp(−500/T) cm^3 molecule^{-1} s^{-1} for HOCl + HO and k(HOCl+O) = 1.0 × 10^{-11} exp(−1300/T) cm^3 molecule^{-1} s^{-1} for HOCl + O, for the low temperature range 200−300 K.

Theoretically, Schindler et al.[7] in 1996 reported that the lowest barrier process in the HOCl + O(^{3}P) reaction is the Cl abstraction by O(^{3}P) through ab initio calculations at the G1//MP2/6-31G(d) level of theory. More recently, Sun's research group[9−11] studied the reaction mechanisms for HOCl reactions with H, O, and HO by G3//MP2/6-311+G(2d,2p) for HOCl +H,[9] CCSD(T)/6-311++G(3df,3dp)//MP2/6-311+G(2d,2p) for HOCl + OH,[10] and G3(MP2)//MPW1K/6-311G(d,p) for HOCl + O.[11] They calculated the rate constants by canonical variational transition state theory on the basis of their predicted reaction pathways and obtained reasonable agreements with the aforementioned experimental data.

To provide rate constants for combustion applications up to 3000 K, we have examined the above three HOCl reactions together with the one involving HO_2, which has shown to be a key product of the HO + ClO_3 reaction.[3b,12] These reactions occurring on their ground state potential energy surfaces have been studied using more accurate quantum chemical methods as described below.

2. Computational Methods

In the present study, the geometric parameters of the species and stationary points related to the four HOCl reactions have been optimized at the BH&HLYP/6-311+G(3df,2p), CCSD/cc-pVDZ, and CCSD/aug-cc-pVDZ levels of theory.[13,15] The moments of inertia and frequencies of all the species and stationary points were calculated with the corresponding optimization methods. For more accurate evaluation of energies,

* Corresponding author. E-mail: chemmcl@emory.edu.

10.1021/jp905136h CCC: $40.75
Published on Web 07/09/2009

higher-level single-point energy calculations of all the species and stationary points have been carried out by the CCSD(T)/6-311+G(3df,2p) and CCSD(T)/aug-cc-pVTZ methods,[13−15] on the basis of the optimized geometries at the BH&HLYP/6-311+G(3df,2p), CCSD/cc-pVDZ, and CCSD/aug-cc-pVDZ levels of theory. Also, for the specific channels of HOCl + O, the G2 M method[16] was used to calculate its single point energy for comparison. All the electronic structure calculations were performed by the Gaussian 03 program.[17]

Rate constant calculations were carried out with the VARIFLEX program[18] based on the microcanonical RRKM (Rice−Ramsperger−Kassel−Marcus) theory[19−21] in temperature range 200−3000 K. Eckart tunneling permeability coefficients[22] were used to correct the rate constants for the hydrogen transfer quantum effects at low temperatures. For a barrierless association/decomposition process, the variational transition state theory (VTST)[23,24] was employed with the fitted Morse function, $V(R) = D_e\{1 - \exp[-\beta(R - R_e)]\}^2$, which represents the minimum potential energy path (MEP). In the $V(R)$ equation, D_e is the binding energy excluding zero-point vibrational energy for an association reaction, R is the reaction coordinate (i.e., the distance between the two bonding atoms), and R_e is the equilibrium value of R at the stable intermediate structure.

3. Results and Discussion

The potential energy surfaces (PESs) of HOCl reactions with H, O(^{3}P), and OH systems were predicted at the CCSD(T)/6-311+G(3df,2p)//BH&HLYP/6-311+G(3df,2p), CCSD(T)/aug-cc-pVTZ//CCSD/cc-pVDZ, and CCSD(T)/aug-cc-pVTZ//CCSD/aug-cc-pVDZ levels of theory, while that of the HOCl + HO_2 reaction was evaluated with the first method only. All PESs are presented in Figure 1. The geometric parameters of all the transition states of the H, O, and OH reactions optimized at the BH&HLYP/6-311+G(3df,2p), CCSD/cc-pVDZ, and CCSD/aug-cc-pVDZ levels of theory and those of the HO_2 reaction computed with the first method are shown in Figure 2. The vibrational frequencies and moments of inertia for the reactants and transition states are summarized in Table 1 for the kinetic calculations. Figure 2 shows that the bond distances at the CCSD/cc-pVDZ level are almost identical with those obtained at the CCSD/aug-cc-pVDZ level, while the maximum difference of the bond lengths between the BH&HLYP/6-311+G(3df,2p) level and the CCSD/aug-cc-pVDZ level is 0.07 Å. In additoin, Figure 1 illustrates the energy difference in the transition states between the CCSD(T)/6-311+G(3df,2p)//BH&HLYP/6-311+G(3df,2p) level and the CCSD(T)/aug-cc-pVTZ//CCSD/aug-cc-pVDZ level; they are less than 1.0 kcal/mol for systems smaller than HOCl + HO_2, for which the CCSD(T)/6-311+G(3df,2p)//BH&HLYP/6-311+G(3df,2p) method was employed.

3.1. HOCl + H. The three potential reaction channels considered for this reaction system are shown in Figure 1A. The lowest barrier channel is Cl abstraction by H to form OH + HCl through a-TS1 with a barrier of 1.6 kcal/mol at the CCSD(T)/aug-cc-pVTZ level. The second channel is the H-for-Cl substitution via transtion state a-TS2 producing H_2O + Cl. The reaction barrier is 5.3 kcal/mol at the CCSD(T)/aug-cc-pVTZ level, which is 3.7 kcal/mol higher than a-TS1. The third channel occurring by a-TS3 is a H-abstraction reaction with the highest barrier of 10.0 kcal/mol in these three reaction channels. Wang et al.[8] calculated two of the transiton states for this reaction at the G3//MP2/6-311+G(2d,2p) level in 2003; their predicted values of a-TS1 and a-TS3 are 1.1 and 10.5 kcal/mol, which agree well with our results, 1.6 and 10.0 kcal/mol, respectively.

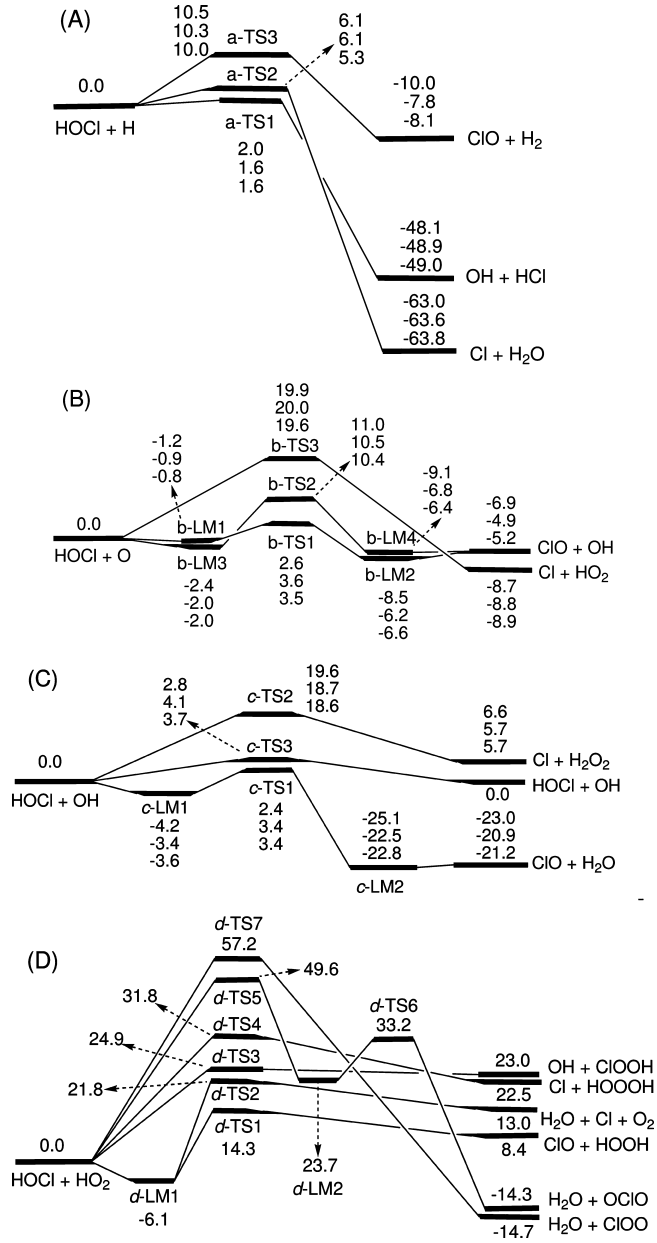

Figure 1. Potential energy profiles of the reaction of HOCl with H/O/OH/HO_2 in units of kcal/mol. The numbers on the top, middle, and bottom lines in (A), (B), and (C) are obtained at CCSD(T)/6-311+G(3df,2p)//BH&HLYP/6-311+G(3df,2p), CCSD(T)/aug-cc-pVTZ//CCSD/cc-pVDZ, and CCSD(T)/aug-cc-pVTZ//CCSD/aug-cc-pVDZ levels of theory, respectively. The numbers in (D) are calculated at the CCSD(T)/6-311+G(3df,2p)//BH&HLYP/6-311+G(3df,2p) level of theory.

From the heats of formation from NIST[25] ($\Delta_f H°_0$(HOCl) = −17.1 ± 0.5 kcal/mol, $\Delta_f H°_0$(H) = 51.6 kcal/mol, $\Delta_f H°_0$(ClO) = 24.2 kcal/mol, $\Delta_f H°_0$(H_2) = 0.0 kcal/mol, $\Delta_f H°_0$(HCl) = −22.0 ± 0.1 kcal/mol, $\Delta_f H°_0$(Cl) = 28.6 kcal/mol, $\Delta_f H°_0$(H_2O) = −57.1 kcal/mol) and Ruscic et al.[26] ($\Delta_f H°_0$(OH) = 8.8 ± 0.1 kcal/mol), the reaction heats of three channels are −10.3 ± 0.5, −47.7 ± 0.7, and −63.0 ± 0.5 kcal/mol for the products ClO + H_2, OH + HCl, and Cl + H_2O, respecitvely. Comparing with the calculated data at the CCSD(T)/6-311+G(3df,2p)//BH&HLYP/6-311+G(3df,2p), CCSD(T)/aug-cc-pVTZ//CCSD/cc-pVDZ, and CCSD(T)/aug-cc-pVTZ//CCSD/aug-cc-pVDZ levels of theory, the literature values agree well with the calculated results for the OH + HCl and Cl + H_2O product channels. But, for the ClO + H_2 product channel, the second

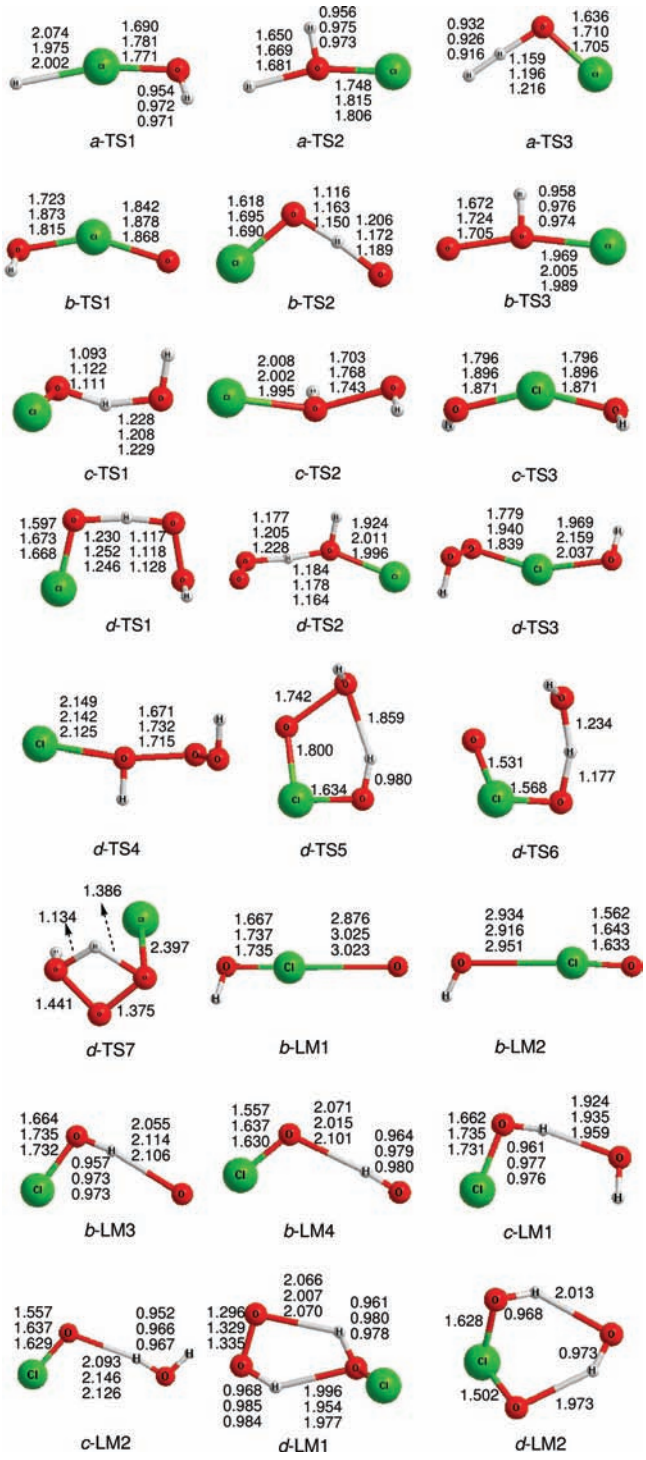

Figure 2. Main geometric parameters (Å) of transition states of the reaction of HOCl with H/O/OH/HO_2. The numbers on the top, middle, and bottom lines are optimized by the BH&HLYP/6-311+G(3df,2p), CCSD/cc-pVDZ, and CCSD/aug-cc-pVDZ methods, respectively. The numbers in d-TS5, d-TS6, d-TS7, and d-LM2 are optimized by the BH&HLYP/6-311+G(3df,2p) method.

and the third calculation methods give smaller exothermicity than the literature estimation by over 2 kcal/mol.

Figure 3A displays the predicted rate constants of the HOCl + H reaction with available literature data. They were predicted with the aforementioned energies and the molecular parameters presented in Table 1 at the CCSD/aug-cc-pVDZ level of theory. The results indicate that the three reaction channels take place with vastly different rates because the barrier at a-TS1 is less than those at a-TS2 and a-TS3 by 3.3 and 6.3 times, respectively. Thus, k_a(a-TS3) is the smallest one even though it appears to have the bigger tunneling effect at low temperatures resulting from its large imaginary frequency (i2182 cm^{-1}) for the H-abstraction process. The total rate constant is contributed mainly from k_a(a-TS1). Comparing with the experimental data at 298 K measured by Ennis and Birks[4] and Vogt and Schindler,[5] our predicted k_a(total) agrees with them quite well. However, the rate constant predicted by Wang et al.[9] in the temperature range of 200−2000 K is noticeably less than our k_a(total) value, especially at high temperatures.

TABLE 1: Vibrational Frequencies and Moments of Inertia Calculated at the CCSD/aug-cc-pVDZ Level of Theory for Reactants and Transition States of HOCl + H/O/HO and at the BH&HLYP/6-311+G(3df,2p) Level of Theory for Reactants and Transition States of HOCl + HO_2

species	I_A, I_B, I_C (au)	frequencies (cm^{-1})
HOCl	2.9, 124.9, 127.9	732, 1299, 3794
	(2.8, 115.6, 118.4)[a]	(810, 1318, 3967)[a]
HO	3.2, 3.2	3715
HO_2	2.7, 51.3, 54.1	1265, 1522, 3835
a-TS1	3.8, 153.0, 156.1	i802, 117, 223, 678, 1219, 3783
a-TS2	3.9, 163.4, 167.4	i1107, 167, 350, 664, 1271, 3770
a-TS3	16.4, 135.1, 151.6	i2182, 385, 619, 744, 1078, 1731
b-TS1	15.5, 380.5, 391.2	i379, 307, 369, 501, 1150, 3781
b-TS2	60.4, 415.6, 476.0	i2949, 152, 540, 595, 754, 867
b-TS3	7.4, 555.8, 563.2	i961, 242, 252, 383, 1226, 3772
c-TS1	62.5, 430.5, 486.3	i2461, 147, 239, 444, 742, 918, 1311, 1632, 3784
c-TS2	19.0, 559.9, 569.0	i848, 207, 310, 410, 513, 1079, 1225, 3777, 3779
c-TS3	21.0, 407.1, 417.0	i245, 286, 426, 431, 482, 1103, 1116, 3771, 3773
d-TS1	145.0, 560.2, 699.7	i2526, 78, 128, 355, 398, 607, 776, 931, 1177, 1495, 1646, 3891
d-TS2	68.8, 1137.9, 1185.3	i3365, 46, 92, 174, 238, 432, 723, 963, 1354, 1460, 1544, 3949
d-TS3	69.3, 695.4, 737.4	i514, 118, 188, 244, 327, 428, 497, 907, 1025, 1504, 3900, 3929
d-TS4	62.6, 1002.0, 1048.6	i729, 69, 166, 242, 256, 417, 542, 1115, 1201, 1528, 3878, 3945
d-TS5	163.5, 418.0, 565.7	i975, 109, 180, 351, 421, 438, 670, 788, 930, 1460, 3474, 3957
d-TS6	189.8, 333.9, 489.4	i2658, 187, 214, 406, 439, 658, 683, 821, 914, 1380, 1766, 3952
d-TS7	150.5, 527.6, 616.8	i1739, 171, 221, 306, 558, 849, 920, 984, 1331, 1533, 2225, 3504

[a] At the BH&HLYP/6-311+G(3df,2p) level of theory.

3.2. HOCl + O(^{3}P). Similar to the HOCl + H system, three O-atom attack channels were considered in the HOCl + O reaction, as shown in Figure 1B. Of these reactions, both Cl- and H-abstraction channels lead to the same products OH + ClO. The former takes place via b-LM1, b-TS1, and b-LM2 with the energies of −0.8, +3.5, and −6.6 kcal/mol, respectively, relative to the reactants predicted at the CCSD(T)/aug-cc-pVTZ level. The latter occurs through b-LM3, b-TS2, and

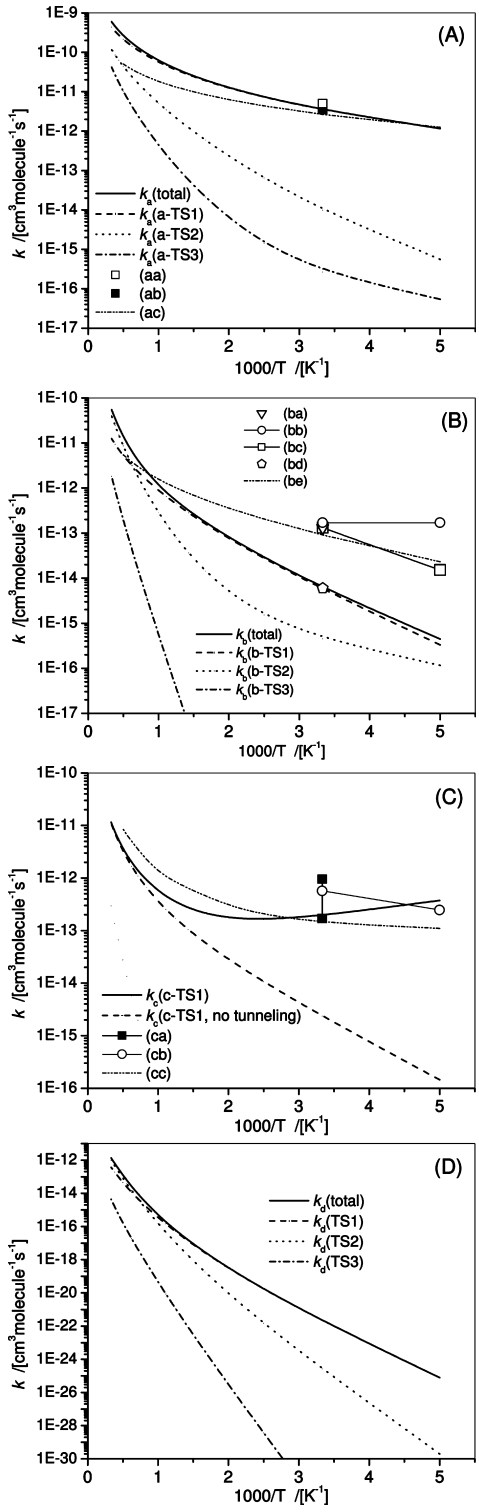

Figure 3. Predicted rate constants and comparison with the data of literature. (A) HOCl + H, (B) HOCl + O, (C) HOCl + OH, and (D) HOCl + HO_2: (aa) ref 4; (ab) ref 5; (ac) ref 9; (ba) ref 6; (bb) ref 7; (bc) ref 8; (bd) ref 25; (be) ref 11; (ca) = (aa) ref 4; (cb) = (bc) ref 8; (cc) ref 10.

b-LM4, similar to the first channel, with the relative energies of −2.0, +10.4, −6.4 kcal/mol, respectively. The energy of b-LM3 is slightly lower than that of b-LM1 while that of b-LM4 is almost equal to that of b-LM2. The transition state b-TS2 is higher than b-TS1 by 6.9 kcal/mol. However, Wang et al.[11] reported the energies at the G3(MP2)/MPW1K/6-311G(d,p) level of theory for these two reaction channels with rather large differences from ours. The energies of four complexes relative to the reactants calculated by Wang et al. are about 3 kcal/mol lower than the values predicted by us. They predicted the barriers of b-TS1 and b-TS2 to be −0.9 and +15.1 kcal/mol, respectively, while Schindler et al.[7] predicted +1.4 and +12.9 kcal/mol, respectively, at the G1//MP2/6-31G(d) level, which are close to our values. Due to the importance of the lowest energy reaction channel via b-TS1, we also performed a series of higher level calculations and sumarized the results in Table 2. It can be seen that the values of b-TS1, calculated by all methods except G3(MP2)//MPW1K/6-311G(d,p), are positive and lie in the range 0−16.8 kcal/mol. CASPT2 and MRCI give the values 4.2 and 6.4 kcal/mol, respectively, which are slightly higher than those calculated by CCSD(T)/aug-cc-pVTZ. G3(MP2)//MPW1K/6-311G(d,p), one of the lowest levels of theory employed, gives the only negative value of b-TS1 (−0.87 kcal/mol), which may be underestimated and questionable.

The third reaction channel of HOCl + O is the substitution of the Cl atom by O via b-TS3 to yield the products Cl + HO_2. The potential energy barrier of this channel at the CCSD(T)/aug-cc-pVTZ level was predicted to be 19.6 kcal/mol, which is close to the result of Schindler et al. (21.0 kcal/mol)[7] at the G1//MP2/6-31G(d) level. Because b-TS3 is higher than b-TS1 by 16.1 kcal/mol and b-TS2 by 9.2 kcal/mol, this substitution channel cannot compete with the abstraction channels.

In addition, from the heat of formation of HOO given by Litorja and Ruscic[34] ($\Delta_f H°_0$(HOO) = 4.0 ± 0.8 kcal/mol) and the above cited literature data, the heats of reaction for the ClO + OH and Cl + HO_2 product channels are computed to be −8.9 ± 0.6 and −9.3 ± 1.3 kcal/mol, respectively. The theoretical values of the ClO + OH channel given in Figure 1B, calculated by CCSD(T)/6-311+G(3df,2p)//BH&HLYP/6-311+G(3df,2p), CCSD(T)/aug-cc-pVTZ//CCSD/cc-pVDZ, and CCSD(T)/aug-cc-pVTZ//CCSD/aug-cc-pVDZ, are 2.0, 4.0, and 3.7 kcal/mol greater than the former (−8.9 ± 0.6 kcal/mol); on the other hand, those of the Cl + HO_2 channel predicted by the three methods are within the error limit of the latter (−9.3 ± 1.3 kcal/mol).

Figure 3A shows the rate constants of the HOCl + O reaction occurring via the three product channels in the range from 200 to 3000 K. Evidently, k_b(b-TS3) is far less than k_b(b-TS1) and k_b(b-TS2), which has a substantially large tunneling effect resulting from its large imaginary frequency of i2949 cm^{-1}. Nevertheless, k_b(b-TS1) is still greater than k_b(b-TS2) below about 1500 K, attributable to the barrier difference of about 7 kcal/mol. But at T > 1500 K, k_b(b-TS2) becomes competitive with k_b(b-TS1). This means that the dominant products, ClO + OH, can be produced by the Cl-abstraction channel at temperatures below 1500 K and by both Cl- and H-abstraction channels over 1500 K.

From Figure 3B, one sees that the predicted k_b(total) is consistent with the estimated value by DeMore and his coauthors[35] but is much less than the experimental data reported by Vogt and Schindler and co-workers[6,7] and the recommended value by Atkinson et al.[8] We notice that the previous theoretical rate constant calculated by Wang et al.[11] agrees well with the recommended value, attributable to the employment of an underpredicted energy barrier at b-TS1 (−0.87 kcal/mol relative to the reactants) with the G3(MP2)//MPW1K/6-311G(d,p) method. However, as stated above and summarized in Table 2, b-TS1 predicted by higher levels of theory are all higher than the reactants, thus giving rise to a noticeably lower value than experimentally measured results. The reason behind the large discrepancy between theory and experiment is not clear at this

TABLE 2: Comparison of Predicted Energies for b-LM1, b-TS1, and ClO + OH by Different Methods

method[a]		relative energy [kcal/mol] to reactants (HOCl + O)		
optimization method	single point correction method	(b-LM1)	b-TS1	ClO + OH
MPW1K/6-311G(d,p)		−2.0	8.5	−3.2
	G3(MP2)//MPW1K/6-311G(d,p)	−6.7	−0.87	−6.2
	G3//MPW1K/6-311G(d,p)	−5.2	0.07	−5.2
	G2M//MPW1K/6-311G(d,p)	−1.5	2.4	−5.1
MPW1K/6-311+G(3df,2p)		−0.74	3.9	−8.3
	G3//MPW1K/6-311+G(3df,2p)	−3.3	1.7	−8.2
	G2M//MPW1K/6-311+G(3df,2p)	−0.60	5.7	−5.0
BH&HLYP/6-311+G(3df,2p)		−0.97	7.3	−7.6
	G3//BH&HLYP/6-311+G(3df,2p)	−2.6	0.21	−7.5
	G2M//BH&HLYP/6-311+G(3df,2p)	−1.2	2.9	−5.6
	CCSD(T)/6-311+G(3df,2p)//BH&HLYP/6-311+G(3df,2p)	−1.2	2.6	−6.8
CCSD/cc-pVDZ		−1.1	16.8	1.4
	CCSD(T)/aug-cc-pVTZ//CCSD/cc-pVDZ	−0.87	3.6	−4.9
CCSD/aug-cc-pVDZ		−0.74	10.7	−1.9
	CCSD(T)/aug-cc-pVTZ//CCSD/aug-cc-pVDZ	−0.82	3.5	−5.2
CASPT2(8,9)/6-311+G(d,p)		−7.2	4.2	−2.4
	MRCI(8,9)+Q/6-311+G(d,p)//CASPT2(8,9)/6-311+G(d,p)	−2.4	6.4	−8.3

[a] MPW1K: ref 27. CASPT2: ref 28. G3: ref 29. G2M: ref 30. MRCI: refs 31 and 32. CASPT2 and MRCI were performed by MOLPRO (ref 33).

point and should perhaps be re-examined in the future experimentally and/or computationally.

3.3. HOCl + OH. In this reaction system, the H-abstracted channel takes place by two H-bonding complexes c-LM1 and c-LM2 and a transition state c-TS1 to form H_2O + ClO. At the CCSD(T)/aug-cc-pVTZ level, c-LM1 and c-LM2 lie below the reactants by 3.6 and 22.8 kcal/mol, respectively, and c-TS1 is above the reactants by 3.4 kcal/mol, which is a bit higher than the value of Wang et al. (2.8 kcal/mol)[10] calculated at the CCSD(T)/6-311++G(3df,3dp)//MP2/6-311+G(2d,2p) level. For the Cl-substitution reaction, the hydroxyl radical attacks the O atom of HOCl to simultaneously undergo the Cl−O bond breaking and the O−O bond forming, giving rise to the products Cl + H_2O_2. This process needs to overcome a higher potential barrier of 18.6 kcal/mol at the CCSD(T)/aug-cc-pVTZ level via the transition state c-TS2, which is much higher than c-TS1 in energy. Actually, there exists a Cl-abstraction channel with a reaction barrier of 3.7 kcal/mol in the HOCl + OH reaction producing OH + ClOH, resulting in the exchange of the OH radicals. Also, based on the heats of formation of H_2O_2 from NIST[25] ($\Delta_f H°_0(H_2O_2) = -31.0$ kcal/mol), the heat of reaction for the Cl + H_2O_2 product channel is 5.9 ± 1.6 kcal/mol, which is very close to the theoretical values, while the heat of reaction for the ClO + H_2O product channel is −24.6 ± 0.7 kcal/mol, which is slightly less than the predicted values shown in Figure 1C.

The predicted rate constants are shown in Figure 3C; k_c(c-TS1) for formation of ClO + H_2O is predominant and is much greater than k_c(c-TS2) for Cl + H_2O_2 production. So, k_c(c-TS2) can be ignored from this figure. Because of the large imaginary frequency, i2461 cm^{-1}, of c-TS1 in the H-abstracton channel, k_c(c-TS1) has a remarkably large tunneling effect at low temperatures. For example, the tunneling effect increases the rate constant by 1700, 68, and 5 times at 200, 300, and 500 K, respectively. However, the effect can be reduced by multiple reflections above c-LM1. For example, at 200 and 300 K, the rate constant is decreased by multiple reflections by a factor of 10 and 1.9, respectively. Combination of these effects leads to a reasonable agreement with experimental data, as shown in Figure 3C. Comparing the result with that of Wang et al.,[10] our evaluations are somewhat higher than theirs in the low temperature and lower in the higher temperature range. Experimentally at 298 K, Ennis and Birks[4] measured the rate constant for HOCl + OH → ClO + H_2O to be $(1.7 - 9.5) \times 10^{-13}$ cm^3 $molecule^{-1}$ s^{-1}, while Atkinson et al.[8] recommended the expression 3.0×10^{-12} exp(−500/*T*) $cm^3 molecule^{-1}$ s^{-1}, for 200−300 K based on the same data, as shown in Figure 3C. Our predicted rate constants are in good agreement with the experimental values.

3.4. HOCl + HOO. This reaction potentially involves more reaction channels as given in Figure 1D predicted only at the CCSD(T)/6-311+G(3df,2p)//BH&HLYP/6-311+G(3df,2p) level of theory because of the limitation of computing resources. The first one is a barrierless association from the reactants to form the intermediate complex d-LM1, which is a five-membered ring structure connected by two hydrogen bonds. This hydrogen bonded complex was predicted to be 6.1 kcal/mol below the reactants and can further decompose to ClO + H_2O_2 and H_2O + Cl + $O_2(^1\Delta_g)$ via d-TS1 and d-TS2, with barriers at 14.3 and 21.8 kcal/mol above the reactants, respectively. The second reaction channel is a direct Cl-abstraction pathway via d-TS3 to yield the HO + ClOOH products. The potential barrier of d-TS3 is 24.9 kcal/mol, which is 3.1 and 10.6 kcal/mol higher than d-TS2 and d-TS1, respectively. The third channel produces Cl + HOOOH by Cl-substitution, whose reaction barrier is higher than d-TS1 by 17.5 kcal/mol. As for the fourth channel, it takes place in two stages via two transition states (d-TS5 and d-TS6) and one intermediate complex (d-LM2) to give the products H_2O + OClO. Because the barrier of the first step is as high as 49.6 kcal/mol, this reaction cannot occur readily in spite of the large reaction exothermicity of 14.3 kcal/mol. Finally, the fifth reaction channel has the highest barrier of 57.2 kcal/mol, suggesting that the rate of production of H_2O + ClOO is negligibly small and can be kinetically ignored.

The heats of reaction for the ClO + H_2O_2, H_2O + OClO, and H_2O + ClOO product channels can be calculated by the heats of formation of OClO and ClOO from NIST[25] ($\Delta_f H°_0$(OClO) = 23.7 ± 1.9 kcal/mol and $\Delta_f H°_0$(ClOO) = 23.8 ± 0.7 kcal/mol), which are +6.3 ± 1.4, −20.4 ± 3.2, and −20.3 ± 2.0 kcal/mol, respectively. From Figure 1D, we can see that ClO + H_2O_2 is theoretically over reactants

by 8.4 kcal/mol, which is close to its reaction heat. But H_2O + OClO and H_2O + ClOO are predicted to be less than the reactants by 14.3 and 14.7 kcal/mol, which are about 6 kcal/mol greater than the values given above. In view of such large deviations, we tried to calculate the heats of reactions for both HOCl + HOO → H_2O + ClOO, and HOCl + HOO → H_2O + OClO by other theoretical methods. For example, at the G2M(cc1)//BH&HLYP/6-311+G(3df,2p) level, the heat of the former reaction is −15.2 kcal/mol and the heat of the latter reaction is −15.7 kcal/mol. At the CCSD(T)/aug-cc-pVTZ//CCSD/aug-cc-pVDZ level, H_2O + ClOO lies at −16.9 kcal/mol, but the relative energy of H_2O + OClO is only −7.3 kcal/mol. This shows that there is a strong electronic relation effect for the radical OClO. It should be treated by the multireference configuration interaction method. Unfortunately, this cannot be done at present because of the limitation in our computational resources. However, both HOCl + HOO → H_2O + ClOO/OClO product channels are not important for the kinetics of the HOCl + HOO reaction due to their high reaction barriers, the question on their theoretical heats of formation may be left for a future study.

For kinetic prediction, we consider only the first two product channels with the lower reaction barriers. Figure 3D shows the predicted rate constants; k_d(d-TS3) for OH + HOOCl formation is much less than k_d(d-TS1) and k_d(d-TS2) for production of ClO + HOOH and H_2O + Cl + $O_2(^1\Delta_g)$, respectively. The imaginary frequencies of d-TS1 and d-TS2 are i2526 and i3365 cm^{-1} at the BH&HLYP/6-311+G(3df,2p) level of theory; these big imaginary frequencies result in the apparent large tunneling effect. Particularly at a low temperature of 200 K, the tunneling transmission coefficients reach 5.51×10^3 and 2.24×10^6 for the ClO + HOOH and H_2O + Cl + $O_2(^1\Delta_g)$ product channels, respectively. However, with increasing temperature, the tunneling effect decreases quickly; for example, at 300, 400, and 500 K, it is predicted to be 90, 15, and 6, respectively, for the former channel and 2.84×10^3, 136, and 27, respectively, for the latter channel. Figure 3D shows that k_d(d-TS1) is much greater than k_d(d-TS2) in the low temperature range because d-TS1 lies below d-TS2 by 7.5 kcal/mol. With increasing temperature, k_d(d-TS1) and k_d(d-TS2) approach each other and cross at about 1400 K, becoming comparable. Therefore, the major products are predicted to be ClO + H_2O_2 at low temperatures and the mixtures of H_2O + Cl + $O_2(^1\Delta_g)$ and ClO + H_2O_2 at high temperatures.

4. Conclusions

Four reactions of HOCl with H, O, HO, and HO_2 have been studied by ab initio quantum chemical calculations with their rate constants predicted by the microcanonical VTST/RRKM theory. Their lowest energy transition states are predicted to be a-TS1 for HOCl + H, b-TS1 for HOCl + O, c-TS1 for HOCl + HO, and d-TS1 for HOCl + HO_2 with the potential barriers of 1.6, 3.5, 3.4, and 14.3 kcal/mol, respectively. The predicted rate constants can be represented by the expressions

$$k_a(\mathrm{HOCl+H}) = 1.01 \times 10^{-16} T^{1.96} \exp(-212/T) \quad (200-3000\ \mathrm{K})$$

$$k_b(\mathrm{HOCl+O}) = 5.50 \times 10^{-21} T^{2.90} \exp(-801/T) \quad (200-3000\ \mathrm{K})$$

$$k_c(\mathrm{HOCl+OH}) = 2.19 \times 10^{-24} T^{3.61} \exp(1351/T) \quad (200-3000\ \mathrm{K})$$

$$k_d(\mathrm{HOCl+HO_2}) = 1.47 \times 10^{-30} T^{5.35} \exp(-3512/T) \quad (200-3000\ \mathrm{K})$$

in units of cm^3 $molecule^{-1}$ s^{-1} in the temperature range 200−3000 K. k_a(HOCl+H) and k_c(HOCl+OH) are in good agreement with the experimental data, whereas k_b(HOCl+O) predicted by the higher levels of theory in the present work was found to be much less than the limited experimental data. In this regard, further improvement in theory and/or experiment is recommended.

Acknowledgment. This work was supported by the Office of Naval Research under grant No. N00014-02-1-0133. Acknowledgment is also made to the Cherry L. Emerson Center of Emory University for the use of its computational resources. M.C.L. gratefully acknowledges the support from Taiwan's National Science Council for a distinguished visiting professorship at the Center for Interdisciplinary Molecular Science, National Chiao Tung University, Hsinchu, Taiwan.

References and Notes

(1) Prasad, S. S. *Plant. Space Sci.* **1976**, *24*, 1187.
(2) Jacobs, P. W. M.; Whitehead, H. M. *Chem. Rev.* **1969**, *69*, 551.
(3) (a) Zhu, R. S.; Lin, M. C. *J. Phys. Chem. C* **2008**, *112*, 14481. (b) Zhu, R. S.; Lin, M. C. In *Energetic Materials, Part 2, Detonation and Combustion*; Politzer, P., Murray, J. S., Eds.; Elsevier Science Publishing: Amsterdam, 2003; Chapter 11, pp 373−443.
(4) Ennis, C. A.; Birks, J. W. *J. Phys. Chem.* **1988**, *92*, 1119.
(5) Vogt, R.; Schindler, R. N. *Ber. Bunsen-Ges. Phys. Chem.* **1993**, *97*, 819.
(6) Vogt, R.; Schindler, R. N. *Geophys. Res. Lett.* **1992**, *19*, 1935.
(7) Schindler, R. N.; Dethlefs, J.; Schmidt, M. *Ber. Bunsen-Ges. Phys. Chem.* **1996**, *100*, 1242.
(8) Atkinson, R.; Baulch, D. L.; Cox, R. A.; Hampson, R. F., Jr.; Kerr, J. A.; Rossi, M.J.; Troe, J. *J. Phys. Chem. Ref. Data,* **1997**, *26*, 521.
(9) Wang, L.; Liu, J. Y.; Li, Z. S.; Huang, X. R.; Sun, C.-C. *J. Phys. Chem. A* **2003**, *107*, 4921.
(10) Wang, L.; Liu, J. Y.; Li, Z. S.; Sun, C.-C. *J. Comput. Chem.* **2004**, *25*, 558.
(11) Wang, L.; Liu, J. Y.; Li, Z. S.; Sun, C.-C. *Chem. Phys. Lett.* **2005**, *411*, 225.
(12) Zhu, R. S.; Lin, M. C. *PhysChemComm* **2001**, *4*, 127.
(13) Scuseria, G. E.; Schaefer, H. F., III. *J. Chem. Phys.* **1989**, *90*, 3700.
(14) Kendall, R. A.; Dunning, T. H., Jr.; Harrison, R. J. *J. Chem. Phys.* **1992**, *96*, 6796.
(15) Pople, J. A.; Head-Gordon, M.; Raghavachari, K. *J. Chem. Phys.* **1987**, *87*, 5968.
(16) Mebel, A. M.; Morokuma, K.; Lin, M. C. *J. Chem. Phys.* **1995**, *103*, 7414.
(17) Frisch, M. J.; Trucks, G. W.; Schlegel, H. B.; Scuseria, G. E.; Robb, M. A.; Cheeseman, J. R.; Montgomery, J. A., Jr.; Vreven, T.; Kudin, K. N.; Burant, J. C.; Millam, J. M.; Iyengar, S. S.; Tomasi, J.; Barone, V.; Mennucci, B.; Cossi, M.; Scalmani, G.; Rega, N.; Petersson, G. A.; Nakatsuji, H.; Hada, M.; Ehara, M.; Toyota, K.; Fukuda, R.; Hasegawa, J.; Ishida, M.; Nakajima, T.; Honda, Y.; Kitao, O.; Nakai, H.; Klene, M.; Li, X.; Knox, J. E.; Hratchian, H. P.; Cross, J. B.; Bakken, V.; Adamo, C.; Jaramillo, J.; Gomperts, R.; Stratmann, R. E.; Yazyev, O.; Austin, A. J.; Cammi, R.; Pomelli, C.; Ochterski, J. W.; Ayala, P. Y.; Morokuma, K.; Voth, G. A.; Salvador, P.; Dannenberg, J. J.; Zakrzewski, V. G.; Dapprich, S.; Daniels, A. D.; Strain, M. C.; Farkas, O.; Malick, D. K.; Rabuck, A. D.; Raghavachari, K.; Foresman, J. B.; Ortiz, J. V.; Cui, Q.; Baboul, A. G.; Clifford, S.; Cioslowski, J.; Stefanov, B. B.; Liu, G.; Liashenko, A.; Piskorz, P.; Komaromi, I.; Martin, R. L.; Fox, D. J.; Keith, T.; Al-Laham, M. A.; Peng, C. Y.; Nanayakkara, A.; Challacombe, M.; Gill, P. M. W.; Johnson, B.; Chen, W.; Wong, M. W.; Gonzalez, C.; Pople, J. A. *Gaussian 03*, revision C.02; Gaussian, Inc.: Wallingford, CT, 2004.

(18) Klippenstein, S. J.; Wagner, A. F.; Dunbar, R. C.; Wardlaw, D. M.; Robertson, S. H. *VARIFLEX version 1.00*; Argonne National Laboratory: Argonne, IL, 1999.
(19) Hase, W. L. *Acc. Chem. Res.* **1983**, *16*, 258.
(20) Wardlaw, D. M.; Marcus, R. A. *Chem. Phys. Lett.* **1984**, *110*, 230.
(21) Klippenstein, S. J. *J. Chem. Phys.* **1992**, *96*, 367.
(22) Eckart, C. *Phys. Rev.* **1930**, *35*, 1303.
(23) Klippenstein, S. J. *J. Phys. Chem.* **1994**, *98*, 11459.
(24) Klippenstein, S. J. *J. Chem. Phys.* **1991**, *94*, 6469.
(25) Chase, M. W., Jr. NIST-JANAF Themochemical Tables, 4th ed. *J. Phys. Chem. Ref. Data*, **1998**, *9*, 1−1951.
(26) Ruscic, B.; Boggs, J. E.; Burcat, A.; Csaszar, A. G.; Demaison, J.; Janoschek, R.; Martin, J. M. L.; Morton, M. L.; Rossi, M. J.; Stanton, J. F.; Szalay, P. G.; Westmoreland, P. R.; Zabel, F.; Berces, T. *J. Phys. Chem. Ref. Data* **2005**, *34*, 573.
(27) Lynch, B. J.; Fast, P. L.; Harris, M.; Truhlar, D. G. *J. Phys. Chem.* **2000**, *104*, 4811.
(28) Celani, P.; Werner, H.-J. *J. Chem. Phys.* **2000**, *112*, 5546.
(29) Baboul, A. G.; Curtiss, L. A.; Redfern, P. C.; Raghavachari, K. *J. Chem. Phys.* **1999**, *110*, 7650.
(30) Mebel, A. M.; Morokuma, K.; Lin, M. C. *J. Chem. Phys.* **1995**, *103*, 7414.
(31) Werner, H.-J.; Knowles, P. J. *J. Chem. Phys.* **1988**, *89*, 5803.
(32) Knowles, P. J.; Werner, H.-J. *Chem. Phys. Lett.* **1988**, *145*, 514.
(33) Werner, H.-J.; Knowles, P. J.; Lindh, R.; Manby, F. R.; Schütz, M.; Celani, P.; Korona, T.; Rauhut, G.; Amos, R. D.; Bernhardsson, A.; Berning, A.; Cooper, D. L.; Deegan, M. J. O.; Dobbyn, A. J.; Eckert, F.; Hampel, C.; Hetzer, G.; Lloyd, A. W.; McNicholas, S. J.; Meyer, W.; Mura, M. E.; Nicklass, A.; Palmieri, P.; Pitzer, R.; Schumann, U.; Stoll, H.; Stone, A. J.; Tarroni, R.; Thorsteinsson, T. *MOLPRO, a package of ab initio programs*, version 2006.
(34) Litorja, M.; Ruscic, B. *J. Electron Spectrosc. Relat. Phenom.* **1998**, *97*, 131.
(35) DeMore, W. B.; Sander, S. P.; Golden, D. M.; Molina, M. J.; Hampson, R. F.; Kurylo, M. J.; Howard, C. J.; Ravishankara, A. R. *JPL Publication 90-1*; Jet Propulsion Laboratory, NASA: Pasadena CA, 1990; p 27.

JP905136H